DOI: 10.1103/PhysRevLett.115.188303

Self-Sustained Density Oscillations of Swimming Bacteria Confined in Microchambers

M. Paoluzzi[1],* R. Di Leonardo[1,2], and L. Angelani[1,3]
[1] *Dipartimento di Fisica Università Sapienza, P.le A Moro 2, 00185 Rome, Italy*
[2] *NANOTEC-CNR, Institute of Nanotechnology, Soft and Living Matter Laboratory, Piazzale A. Moro 2, I-00185, Roma, Italy*
[3] *Istituto dei Sistemi Complessi (ISC-CNR), UOS Sapienza, P.le A Moro 2, 00185 Rome, Italy*

We numerically study the dynamics of run-and-tumble particles confined in two chambers connected by thin channels. Two dominant dynamical behaviors emerge: (*i*) an oscillatory pumping state, in which particles periodically fill the two vessels and (*ii*) a circulating flow state, dynamically maintaining a near constant population level in the containers when connected by two channels. We demonstrate that the oscillatory behaviour arises from the combination of a narrow channel, preventing bacteria reorientation, and a density dependent motility inside the chambers.

arXiv:1412.1131v2 [cond-mat.soft] 3 Nov 2015

Introduction.— Self-sustained oscillators are ubiquitous in physics and biology [1]. From the Van der Pol oscillator to the heartbeat these systems are characterised by a periodic motion that is sustained against dissipation by some form of energy source. Active systems constantly consume an internal energy source to sustain persistent motions in a highly dissipative environment [2, 3]. This results in a strongly out of equilibrium dynamics that can give rise to unidirectional actuation of micro-objects [4–7], spontaneous accumulation of passive colloids over target sites [8], long lived density fluctuations [9–11], large-scale vortex lattice [12], frozen steady states [13], active liquid crystals [14] or macroscopic directed motion [15]. It has been shown that the large scale collective patterns that spontaneously break and reform in many active systems can be stabilized by confining microstructures [16–18]. However spatial confinement always results in long lived unidirectional flows that only rarely and randomly can switch direction [18].

In this Letter we investigate the possibility of using geometric confinement to obtain self-sustained oscillations in active matter systems. In particular, by using numerical simulations, we show that active particles can alternately fill and empty two micro chambers connected by thin channels. We find that the number of particles inside each chamber fluctuates with a distribution that becomes increasingly bivariate for large particle densities. The narrowness of the channels ensures single file dynamics [19–24] and inhibits cell reorientation. This, together with a density dependent motility of swimmers inside the chambers, gives rise to the observed oscillatory behavior. In addition, when the chambers are connected by two channels we observe also a circulating flow maintaining a near constant population level in the containers.

Results and discussion.— We perform Molecular Dynamics simulations of N run-and-tumble swimmers [25–28] of length ℓ and thickness a, with $a/\ell = 1/2$, in two dimensions [4, 29, 30]. The interaction between the swimmers is purely repulsive. The system is confined in two chambers connected by one or two channels. Details of the model can be found in [31].

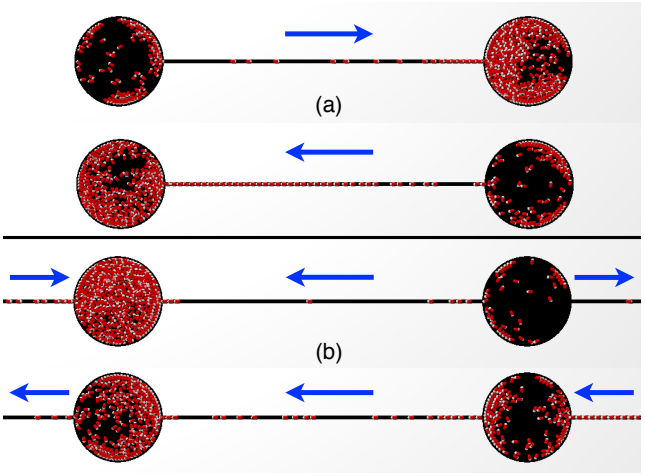

FIG. 1: Snapshots of the simulations of active particles confined in two chambers connected by thin channels. Panel (a): alternating pumping, in which particles alternately fill and empty the chambers in the case of a single channel. Panel (b): alternating pumping and circular flow in the case of two channels connecting the chambers.

We first consider two circular chambers of radius $R=7\ell$ connected by a thin channel of length $L=50\ell$ and transverse size $\sigma = \ell/2$ (see Fig. (1), panel (a)). The total number of particles N was varied from 160 to 464 corresponding to area fractions ϕ going from 0.21 to 0.62 [34]. We found that the presence of persistent currents in thin channels gives rise to large fluctuations in particle distributions between the two chambers. The symmetric state, where the two chambers are equally populated, becomes unstable due to the spontaneous formation of large currents with a characteristic lifetime that increases with the total number of swimmers. As a consequence, one of the two chambers is progressively filled with particles up to a point where it triggers the formation of a

reversed current. This mechanism gives rise to an oscillatory pumping between the two containers as evidenced in the snapshots of the numerical simulations (panel (a), Fig. (1) and the movie in [31]). In Fig. (2a) the time evolution of the fraction of particles in the two reservoirs $n_{1,2}$ are shown for a sample run with $\phi = 0.47$. Fig. (2b) shows the corresponding channel current defined as the sum of the velocities of particles inside the channel, $j = \sum_k' v_k(t)/L$. A clear oscillation is observed with a period of about 2000. In the following we will consider the probability distribution for coarse grained variables $P(x)$ and $P(x,y)$, defined as $P(x) \equiv \overline{\langle \delta(x - x(t)) \rangle}$ and $P(x,y) \equiv \overline{\langle \delta(x - x(t))\delta(y - y(t)) \rangle}$ where $\overline{\cdots}$ indicates the time average and the angular brackets $\langle \ldots \rangle$ averages over 120 independent runs. Calling $\delta n = n_2 - n_1$ the asymmetry parameter, we compute the joint probability density $P(\delta n, j)$ and the power spectrum $S(\omega) = |\delta\hat{n}(\omega)|^2$, with $\delta\hat{n}(\omega)$ the Fourier transform of $\delta n(t)$. In the upper panels of Fig. (3) the quantity $P(\delta n, j)$ is shown for $\phi = 0.30$ and $\phi = 0.47$. Contrary to the case of passive thermal particles, where a stable equilibrium point exists at ($\delta n = 0$, $j = 0$), here we observe a stationary limit cycle corresponding to fluxes that alternately empty and fill the containers (a video of a typical trajectory followed by the system in the $(\delta n, j)$ plane is shown in Supplemental Material [31]. This oscillating behaviour appears as a peak in the power spectrum $S(\omega)$ (Fig. (3)d). The high frequency behavior of $S(\omega)$ is well approximated by a $\sim \omega^{-2}$ tail (the solid black lines in Fig. (3)d), indicating that the dynamics of $\delta n(t)$ is uncorrelated on small time-scales. When the number of particles is increased, it takes a longer time to fill or empty the chambers resulting in a decrease of the peak frequency. For high particle densities δn displays fluctuations that are large and long lived as shown by the pronounced peaks at $\delta n \sim \pm 1$ in $P(\delta n, j)$ (Fig. 3b). The two chambers alternately fill and empty almost completely although transitions between these two states lose periodicity and the peak in $S(\omega)$ disappears (Fig. 3d).

In order to analyze in more details the role played by the swimmers density we investigate the behavior of $P(\delta n)$ at different particles number. As one can see in panel (c) of Fig. (2), the distribution $P(\delta n)$ becomes bimodal by increasing ϕ. The bimodality of $P(\delta n)$ indicates that density oscillations take place between two high density and long lived states, as a result the two chambers are alternatively almost filled and $\delta n \to \pm 1$. The quantity δn_{max}, defined as the value of $|\delta n|$ where the distribution reaches its maximum value, continuously grows with ϕ, up to the threshold value $\phi = 0.47$. For higher densities one of the two chambers fills up completely and the corresponding internal motility vanishes [31] giving rise to long lived jammed states (the grey area in Fig. 3c). Varying the channel length L from 50ℓ to 25ℓ, at least in the analyzed range, seems to have little effects on the results [31]. Performing simulations at different channel size $\sigma/\ell = 1/2, 1, 3/2, 2$ (with $L/\ell = 25, 50$ and for the case $\phi = 0.47$, i.e. where $P(\delta n)$ is strongly bimodal) we observe that δn_{max} decreases toward 0 by increasing σ, indicating that the channel thickness plays a crucial role in the observed alternate pumping phenomenon [31].

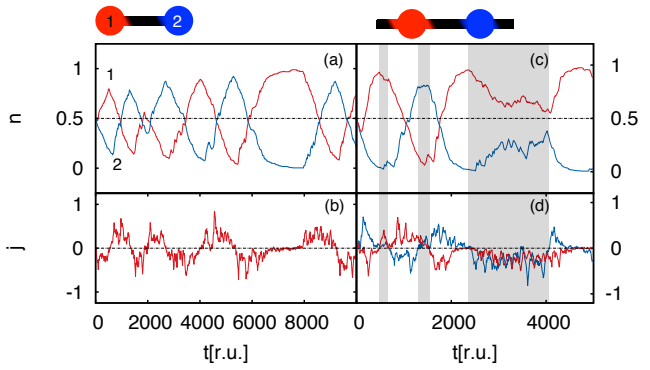

FIG. 2: Time evolution of the fraction of swimmers $n_{1,2}(t)$ inside the vessels and the channel current $j(t)$ for a typical single run. Left panels refer to the case of one channel ($\phi = 0.47$), while right panels to the case of two channels ($\phi = 0.44$). In panel (d) the currents of the first and second channel are reported and grey area correspond to concordant currents, $j_1 \cdot j_2 > 0$.

At the microscopic level the mechanism responsible for the observed phenomenology relies on the fact that particles in a thin channel are unable to reverse their direction of motion, thus forming long files of pushing bacteria. A small difference in the number of left and right oriented bacteria determines the sign of the net flux, and counter-current swimming bacteria are then pushed back to their original chamber, with a consequent increase of the net flux in the channel. As a result small fluctuations are amplified, giving rise to long lived flows of particles in the system. For non interacting particles, the rate of bacteria passing from one chamber to the channel will be simply proportional to the number of bacteria in the chamber N_i with $i = 1, 2$ the chamber index. Because of interactions, when the number of particles in the chamber is near to close packing N_0, the motility will be reduced with a consequent reduction in the entrance rate [31]. A simple form for the rate that is consistent with this behaviour is $\alpha = \beta N_i(1 - N_i/N_0)$. The rate of entrance in the channel is also affected by the sign of j that makes it harder for bacteria to enter a channel when there's a counter-flowing current. To account for this last observation we suppose that β can assume two different values β_+, β_- according to the sign of the current j. We found that the above expression for α fits very well our simulation data Fig. (4) panel (a). The origin of the oscillating behaviour becomes now clear if one follows the time evolution of $N_{1,2}$ over the curves in Fig. (4,a). Let's start from the case where the total number of particles N is

less than N_0 and bacteria are equally distributed in the two chambers. Due to the narrowness of the channel, bacteria will conserve their direction from the moment they enter the channel until they exit. A current reversal, for example from positive to negative, can then be triggered only if the rate of left going bacteria entering from the right chamber is higher than the number of right going bacteria entering from the left chamber. If we assume an initial positive current than the left chamber will loose bacteria and N_1 will move on the upper curve in Fig. (4,b) towards left. Since the total number of particles has to be conserved N_2 will move symmetrically on the lower curve towards right. This flow of bacteria from the left chamber to the right chamber will continue until there's a higher chance for bacteria to enter the channel from the right and trigger a current reversal. At this point N_1 will move on the lower curve, N_2 on the upper curve and a reversed cycle will occur. When the total number of particle is equal to N_0, N_1 and N_2 will start from the middle of the graph (Fig. (4) panel c) and the two rates α will only become equal when one structure is full and the other is empty and both values of alpha vanish. At this point a current reversal can only occur by an unbiased random fluctuation and the process is reversed with no defined period. This simple picture quantitatively describes the observed increase of oscillation amplitudes with increasing ϕ (see inset in Fig.3c).

We now consider the case in which two channels connect the chambers. Performing numerical simulations at different particles area fractions ϕ, from 0.20 to 0.58 [34], we observe two dominant behaviors – see snapshots in panel (b) of Fig. (1) and the movies in [31]. The first one is the oscillatory pumping of swimmers between the two chambers – top of panel (b) in Fig. (1) – in analogy with what observed in the presence of one channel. Again, differently from the equilibrium case, the fraction of particles in the containers is affected by strong fluctuations that favour flows that alternately empty and fill the chambers. The presence of the second channel has the effect of reinforce the flows, resulting in higher peak frequencies (shorter oscillation times) with respect to the one-channel case. The second new behavior, forbidden by construction when only one channel connects the chambers, is a circular flow of swimmers in the system. In such a case the currents j_1 and j_2 in the two channels have the same orientation and the number of particles n_1 and n_2 inside the chambers turn out to be nearly constant. This circulating flow persists until a fluctuation in the number of right and left oriented particles in a channel gives rise to an inversion of the flux, thus resulting in two channel flows pointing towards the same chamber falling back into the previous situation of oscillatory pumping behavior. This kind of intermittent behavior between the two phases is made clear by looking at the

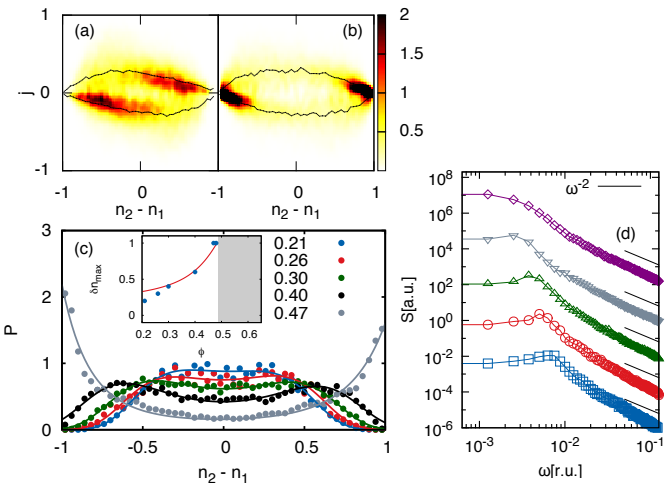

FIG. 3: Single channel. Top panels: the join probability $P(n_2-n_1,j)$ at two different densities, $\phi = 0.30$ (panel (a)) and $\phi = 0.47$ (panel (b)). Panel (c): probability distribution function $P(n_2-n_1)$ increasing the number of swimmers for $L = 50\ell$ and $\sigma = \ell/2$. The full lines are fits with $f(\delta n) = \exp(a+b\delta n^2+c\delta n^4)$. Inset: δn_{max} (blue symbols) as a function of ϕ, the red line is the amplitude of the oscillations predicted by the model. Densities in the grey area correspond to jammed states where all bacteria fill one of the two chambers almost completely. Panel (d): power spectrum $S(\omega)$ at five different densities. For clarity the individual curves have been vertically shifted multiplying for 10^{2n} with $n = 0, ..., 5$. The corresponding area fractions ϕ are (from bottom to top) 0.21 (blue symbols), 0.26 (red), 0.30 (green), 0.40 (grey) and 0.47 (purple).

time evolution of n_i and j_i – see as example the reported case in Fig. 2, panel (c) and (d). When j_1 and j_2 have the same sign, $j_1 \cdot j_2 > 0$, a circular flow sets in (grey area in the figure), with a nearly constant population level in the two containers. In the case $j_1 \cdot j_2 < 0$ swimmers flow into the same box, increasing its population level until a reverse flux pumps out particles from it and fills the other container (white area in the figure). The existence of circulating flows and oscillatory pumping is also evident by looking at the joint probability densities $P(j_1+j_2,\delta n)$ and $P(j_1-j_2,\delta n)$. Circulating flows correspond to the two spots of $P(j_1+j_2,\delta n)$ at $\delta n \sim 0$ and $j_1+j_2 \neq 0$ (Fig. (5)a) and to the single spot of $P(j_1-j_2,\delta n)$ at the origin (Fig. (5)b). The oscillatory behavior produces, instead, accumulation of particles into the chambers, producing the spots at $\delta n \sim \pm 1$.

The role of swimmers density is analyzed by studying the ϕ-dependence of the probability density $P(j_1+j_2)$. We observe that $P(j_1+j_2)$ changes its shape by increasing ϕ, developing a three peaks structure at high densities, $\phi > 0.24$ – Fig. (5), panel c. The two peaks at $j_1+j_2 \neq 0$ are due to the circulating flows. The peak in zero corresponds to the limiting situations of maximum density unbalance produced by the alternating pumping

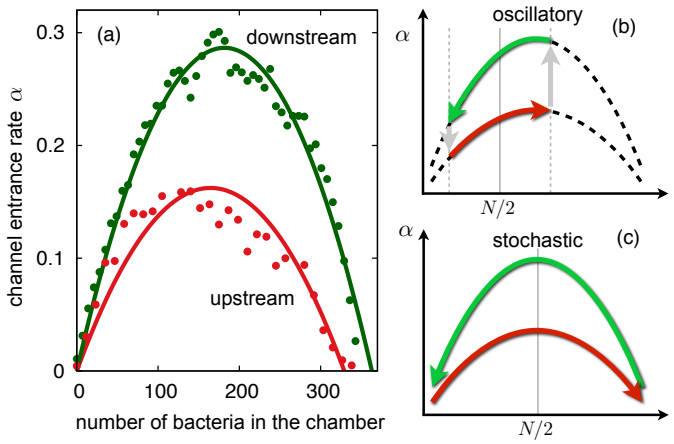

FIG. 4: Left panel: variation of the number of swimmers in the channel as a function of N_i for downstream (green symbols) and upstream (red symbols). The full lines are the fits with α. Right panels: the sketch of the mechanism responsible of the alternating pumping for the oscillatory regime (top) and in the case of the stochastic regime (bottom), i. e., when the current is reversed with no defined period.

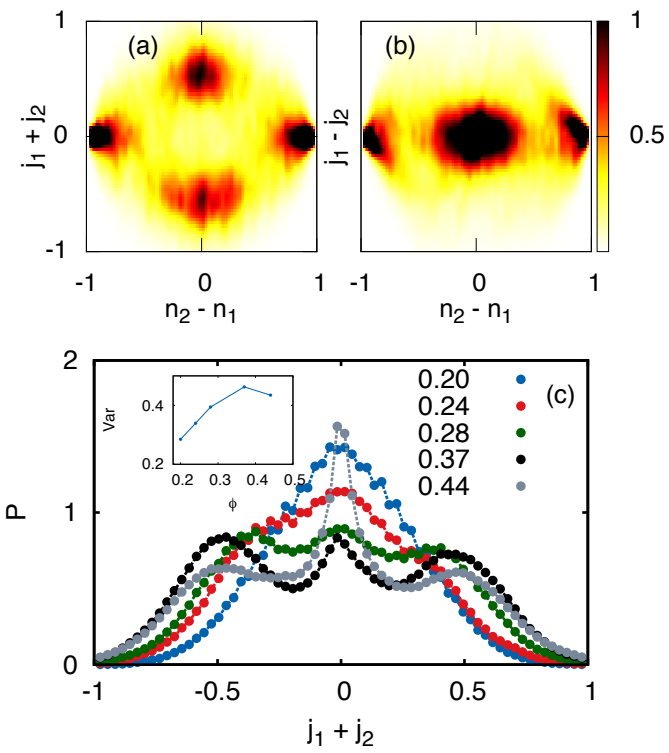

FIG. 5: Double channel. Top panels: the join probabilities $P(j_1+j_2, \delta n)$ (panel (a)) and $P(j_1-j_2, \delta n)$ (panel (b)) for $\phi = 0.44$. Panel (c): probability distribution function $P(j_1+j_2)$ increasing the number of swimmers for $L = 50\ell$ and $\sigma = \ell/2$. Inset: variance of the distribution $P(j_1+j_2)$ as a function of ϕ for $L = 50\ell$ and $\sigma = \ell/2$.

state (the spots at $\delta n \sim \pm 1$ and $j_1 + j_2 \sim 0$ in panel (b) Fig. (5)). This central component increases with particle density producing a non monotonic behaviour in the variance of $P(j_1+j_2)$ as a function of ϕ (see the inset in Fig. (5)c). Changing the chamber size at fixed density does not have relevant effects on the reported behavior [31].

Conclusions.— We have shown that confining active particles in micro-chambers connected by thin channels gives rise to self-sustained density oscillations, alternately filling the two containers. When adding a second channel, this oscillatory behaviour is still present together with circulating flows. The basic ingredients of such an effect are a density dependent motility combined with the narrowness of the channels, which only permits single file dynamics and inhibits cell reorientation. The reported numerical findings suggest a possible route to generate self-sustained oscillations in active matter. The proposed mechanism could be investigated experimentally since bacteria such as *E. coli* and *B. subtilis* remain motile even when constrained in thin channels with a size that is comparable to their diameter [35, 36].

We acknowledge support from MIUR-FIRB project RBFR08WDBE. RDL acknowledges funding from the European Research Council under the European Unions Seventh Framework Programme (FP7/2007-2013)/ERC grant agreement No. 307940.

* Electronic address: matteo.paoluzzi@ipcf.cnr.it

[1] A. Pikovsky, M. Rosenblum, and J. Kurths, *Synchronization - A Universal Concept in Nonlinear Sciences* (Cambridge University Press, Cambridge, England, 2001).
[2] H. C. Berg, *E. Coli In Motion* (Springer, New York, 2004).
[3] M. C. Marchetti *et al.*, Rev. Mod. Phys. **85**, 1143 (2013).
[4] L. Angelani, R. Di Leonardo and G. Ruocco, Phys. Rev. Lett. **102**, 048104 (2009).
[5] L. Angelani and R. Di Leonardo, Comp. Phys. Commun. **182**, 1970 (2011); New J. Phys. 12, 113017 (2010).
[6] R. Di Leonardo, *et al.*, Proc. Natl. Acad. Sci. **107**, 9541 (2010).
[7] A. Sokolov, *et al.*, Proc. Natl. Acad. Sci. U.S.A. **107**, 969 (2010).
[8] N. Koumakis, *et al.*, Nature Communications, **4**, 2588 (2013).
[9] V. Narayan, S. Ramaswamy, and N. Menon, Science **317**, 105 (2007).
[10] J. Toner, and Y. Tu, Phys. Rev. Lett. **75**, 4326 (1995). Phys. Rev. E **58**, 4828 (1998). J. Toner, Y. Tu, and S. Ramaswamy, Ann. Phys. **318**, 170 (2005).
[11] S. Ramaswamy, R. A. Simha, and J. Toner, Europhys.

Lett. **62**, 196 (2003).
[12] Y. Sumino *et al.* Nature **483**, 448 (2012).
[13] V. Schaller, *et al.*, Proc. Natl. Acad. Sci. U.S.A. **108**, 19099 (2011).
[14] S. Zhou, *et al.*, Proc. Natl. Acad. Sci. U.S.A. **111**, 1265 (2014).
[15] A. Bricard, J.-B. Caussin, N. Desreumaux, O. Dauchot, and D. Bartolo, Nature **503**, 95 (2013).
[16] T. Sanchez, *et al.*, Nature **491**, 431 (2012).
[17] H. Wioland, F.G. Woodhouse, J. Dunkel, J.O. Kessler, and R.E. Goldstein Phys. Rev. Lett. **110**, 268102 (2013).
[18] O. Sipos, K. Nagy, and P. Galajda, Chem. Biochem. Eng. Q. **28**, 233 (2014).
[19] A. Jelić *et al.* Eur. Phys. Lett. **98**, 40009 (2012).
[20] P. Illien *et al.* Phys. Rev. Lett. **111**, 038102 (2013).
[21] M. Gorissen *et al.* Phys. Rev. Lett. **109**, 170601 (2012).
[22] I. Neri *et al.* Phys. Rev. Lett. **110**, 098102 (2013).
[23] E. Locatelli, M. Pierno, F. Baldovin, and E. Orlandini, Phys. Rev. E **91**, 022109 (2015).
[24] Q. H. Wei, C. Bechinger, and P. Leiderer, Science **287**, 625-627 (2000).
[25] M. B. Wan, C.J. O. Reichhardt, Z. Nussinov, and C. Reichhardt, Phys. Rev. Lett. **101**, 018102 (2008).
[26] M. J. Schnitzer, Phys. Rev. E **48**, 2553 (1993).
[27] M. E. Cates, Rep. Prog. Phys. **75**, 042601, (2012).
[28] J. Tailleur, and M. E. Cates, Phys. Rev. Lett. **100**, 218103 (2008).
[29] L. Angelani, A. Costanzo and R. Di Leonardo, EPL **96**, 68002 (2011).
[30] M. Paoluzzi, R. Di Leonardo, and L. Angelani, J. Phys.: Condens. Matter **25** 415102 (2013); J. Phys.: Condens. Matter **26** 375101 (2014).
[31] Supplemental material, which includes Refs. [32] and [33].
[32] S. Kim and S. Karrila, *Microhydrodynamics* (Dover, New York, 2005).
[33] L. Angelani, EPL 102, 20004 (2013).
[34] The area fraction ϕ is calculated as NA_s/A where $A_s = \pi(l/4)^2+l^2/4$ is the cross section of a single spherocylindrical swimmer and $A=2\pi R^2+\sigma L$ is the total available area ($A=2\pi R^2+2\sigma L$ in the case of the double channel).
[35] S. A. Biondi, *et al.* AICHE J **44**, 1923 (1998).
[36] J. Mannik *et al.*, Proc. Natl. Acad. Sci. U.S.A. **106**, 1468 (2009).